

南太行山平顺辉长岩体锆石 SHRIMP U-Pb 年龄、 地球化学特征及构造意义^{*}

杨金昆, 张海东^{**}, 刘建朝, 彭素霞, 王得权

(长安大学地球科学与资源学院, 陕西 西安 710064)

摘要 南太行山平顺辉长岩体主要造岩矿物为斜长石、单斜辉石、普通角闪石和橄榄石等。锆石 SHRIMP U-Pb 同位素定年结果表明, 辉长岩体形成于(123.4±1.7)Ma, 为早白垩世华北板块内岩浆活动的产物。平顺辉长岩 $w(\text{SiO}_2)$ 为 42.82%~49.74%, $w(\text{Al}_2\text{O}_3)$ 为 11.91%~16.54%, $w(\text{MgO})$ 为 6.79%~14.57%, $w(\text{TiO}_2)$ 为 0.36%~1.53%, $w(\text{Fe}_2\text{O}_3^{\text{T}})$ 为 4.02%~15.03%, $w(\text{CaO})$ 为 7.45%~18.70%, $w(\text{K}_2\text{O}+\text{Na}_2\text{O})$ 为 2.42%~3.81%, $\text{Mg}^#$ 为 56.53~81.68, LREE 富集, HREE 亏损, 略显微弱的正 Eu 异常, 以富集 LILE、LREE 元素和亏损 Nb-Ta 等高场强元素为特征。辉长岩 $^{206}\text{Pb}/^{204}\text{Pb}$ 为 17.062~18.295, $^{207}\text{Pb}/^{204}\text{Pb}$ 为 15.354~15.422, $^{208}\text{Pb}/^{204}\text{Pb}$ 为 37.185~37.298, I_{Sr} 为 0.7046~0.7051, $\varepsilon_{\text{Nd}}(125 \text{ Ma})$ 为 -14.03~-13.00, 表明平顺辉长岩起源于 EM I 富集地幔, 并受到少量地壳物质的混染, 可能是早白垩世华北克拉通破坏事件在太行山地区的岩浆活动产物。

关键词 地球化学; 岩浆活动; EM I ; 平顺辉长岩; 南太行山

中图分类号:P588.12⁴

文献标志码:A

SHRIMP U-Pb dating, geochemistry and tectonic implications of Pingshun gabbros in southern Taihang Mountain

YANG JinKun, ZHANG HaiDong, LIU JianChao, PENG SuXia and WANG DeQuan

(Chang'an University, Xian 710054, Shaanxi, China)

Abstract

The major petrogenetic minerals in the Pingshun gabbros located in southern Taihang Mountain are plagioclase, clinopyroxene, hornblende and olivine. As the SHRIMP zircon U-Pb dating results show, diagenetic age of gabbros is (123.4±1.7) Ma, which indicates that the gabbros were formed by Early Cretaceous magmatism in the North China craton. The major oxides of the Pingshun gabbros are $w(\text{SiO}_2)$ 42.82%~49.74%, $w(\text{Al}_2\text{O}_3)$ 11.91%~16.54%, $w(\text{MgO})$ 6.79%~14.57%, $w(\text{TiO}_2)$ 0.36%~1.53%, $w(\text{Fe}_2\text{O}_3^{\text{T}})$ 4.02%~15.03%, $w(\text{CaO})$ 7.45%~18.70%, $w(\text{K}_2\text{O}+\text{Na}_2\text{O})$ 2.42%~3.81% and $\text{Mg}^#$ 56.53~81.68. LREE are enriched, and HREE are depleted, coupled with no or a weak positive Eu anomalies. Moreover, the rocks are characterized by high abundances of LILE and LREE, and low abundances of HFSE (such as Nb and Ta). The $^{206}\text{Pb}/^{204}\text{Pb}$ ratios of gabbros range from 17.062 to 18.295, $^{207}\text{Pb}/^{204}\text{Pb}$ ratios from 15.354 to 15.422, and $^{208}\text{Pb}/^{204}\text{Pb}$ ratios from 37.185 to 37.298. $I_{\text{Sr}}=0.7046\sim0.7051$ and $\varepsilon_{\text{Nd}}(125 \text{ Ma})=-14.03\sim-13.00$. These data suggest that Pingshun gabbroic magma originated from the EM I, and was contaminated by minor crustal composition. Hence it might have been formed by early Cretaceous mag-

* 本文得到国家自然科学基金(编号:41040020, 41073027)和中央高校基金(编号:CHD2011ZY005, CHD2011JC168)的联合资助
第一作者简介 杨金昆,男,1995 年生,硕士研究生,岩石学、矿物学、矿床学专业。Email: 981504143@qq.com

** 通讯作者 张海东,男,1982 年生,博士,副教授,主要从事岩石学、地球化学和矿床学研究。Email:270409938@qq.com
收稿日期 2016-05-25; 改回日期 2018-06-01。秦思婷编辑。

matism in Taihang Mountain area resulting from the destruction of the North China Craton.

Key words: geochemistry, magmatism, EM I , Pingshun gabbros, the southern Taihang Mountain

华北克拉通岩石圈在中生代发生了大规模减薄作用，并伴随大规模岩浆活动和成矿作用，但在岩石圈减薄的机制和范围等问题上，尚没有形成统一的认识，并存在较大的争议。太行山构造岩浆岩带不仅是中国东、西部重力梯度带，还是地壳厚度突变地带，很多学者将其作为中国东部岩石圈减薄的边界(Xu, 2007)，但也有一部分学者对这一认识提出了其他看法(吴福元等, 2003; 2006; 2008)。要解决这一问题，很显然需要对太行山地区幔源岩体的形成年代和成因进行深入研究。目前对于基性岩体的成因主要存在3种观点：一种认为该类岩石起源于富集型的岩石圈地幔(许文良等, 2003)，并受到了陆壳物质的混染(Chen et al., 2003)；另一种认为该类岩石的岩浆起源于陆壳物质改造的岩石圈地幔的部分熔融(Wang et al., 2006)；第三种认为该类岩石是壳幔岩浆混合的产物(Chen et al., 2008)。

太行山地区基性岩体出露较少，主要分布在平顺、符山和王安镇等地区。本文研究区(平顺地区)研究工作相对薄弱。Xu等(2010)在辉长岩体中发现了纯橄榄岩地幔包体和橄榄石捕虏晶，认为这代表了受到富Si流体改造的太古代岩石圈地幔的残留。王春光等(2011)对西安里辉长岩进行了LA-ICP-MS锆石U-Pb定年和Hf同位素组成研究，发现辉长岩体形成于131 Ma，并认为辉长岩是拆沉的陆壳物质熔融的熔体与地幔橄榄岩反应的产物。刘建朝等(2009)通过对平顺岩体岩石学、地球化学和Pb同位素研究，提出壳幔岩浆混合成因的看法。上述研究的共同点就是都认为岩浆起源于地幔，并有地壳物质的加入，但关于壳源物质的加入量以及加入过程等问题尚不是很清楚，故有必要对辉长岩年代学和Sr-Nd-Pb同位素组成开展进一步研究，这些研究可以为正确地认识南太行山地区、甚至整个华北克拉通内部中生代岩浆作用的时空分布、岩石圈的减薄机制和范围提供重要依据。本文将通过对平顺辉长岩体岩石学、年代学、主微量元素和Sr-Nd-Pb同位素组成的详细研究，获取平顺辉长岩体源区特征和成因信息，为约束和探讨华北克拉通岩石圈减薄的范围提供新证据。

1 地质背景及岩石学特征

平顺辉长岩体位于华北克拉通内部太行山中生代构造岩浆岩带南段(图1)。研究区发育太古代或古元古代的基底地层，1.85 Ga左右华北东部陆块和西部陆块发生碰撞拼合，形成碰撞造山带，在1.85~0.2 Ga之间发生稳定持续沉积，形成古生代碳酸盐岩盖层，中生代发生强烈构造岩浆作用(吴福元等, 2008)。

平顺辉长岩体呈岩株产出，面积较小，约1.5 km²左右，呈侵入接触分布于闪长岩体内部(图1)。岩体呈黑色-深黑绿色，辉长结构，块状构造，球状分化较普遍(图2a)。主要组成矿物为斜长石(28%~38%)、单斜辉石(15%~35%)、普通角闪石(10%~25%)、橄榄石(5%)以及少量斜方辉石和黑云母。斜长石呈短柱状，发育聚片双晶，牌号为55~65，属偏基性斜长石；单斜辉石呈淡绿色至绿色，半自形柱状，明显被角闪石交代；角闪石呈半自形-自形柱状，少量具有辉石外形，可见绿泥石化，部分被黑云母交代；橄榄石呈港湾状，裂理发育，蛇纹石化发育(图2b~d)。

2 样品采集及分析方法

本次工作岩石样品分别采自于平顺辉长岩体出露的3个地段内(图1)，其中，用于测年的样品(LG01)采自于卢沟地段的采石场内(图1)。样品采回后，首先采用人工重砂法从新鲜岩石样品中分选出锆石，然后在双目镜下挑选出干净、透明、完整的自形锆石颗粒，与标样锆石一并镶嵌于树脂中。后经打磨、抛光、镀金，完成锆石的制靶工作。锆石测年工作在中国地质科学院地质矿产所离子探针中心完成，分析流程详见文献(Compston et al., 1984; Williams et al., 1987; 宋彪等, 2002等)。锆石U、Th、Pb含量测试值，需要用标准斯里兰卡锆石SL13($w(U)=238 \times 10^{-6}$, $t=572$ Ma)进行校正。采用Ludwing SQUID1.0(2001)及ISOPLT(1999)程序对锆石测试数据进行处理，年龄计算采用IUGS(1977)的推荐值。样品全岩的主量元素和Pb同位素测试工作在中国科学院广州地球化学研究所完成，主量元素采用XRF测试，Pb同位素采用MAT262 TIMS测试。微

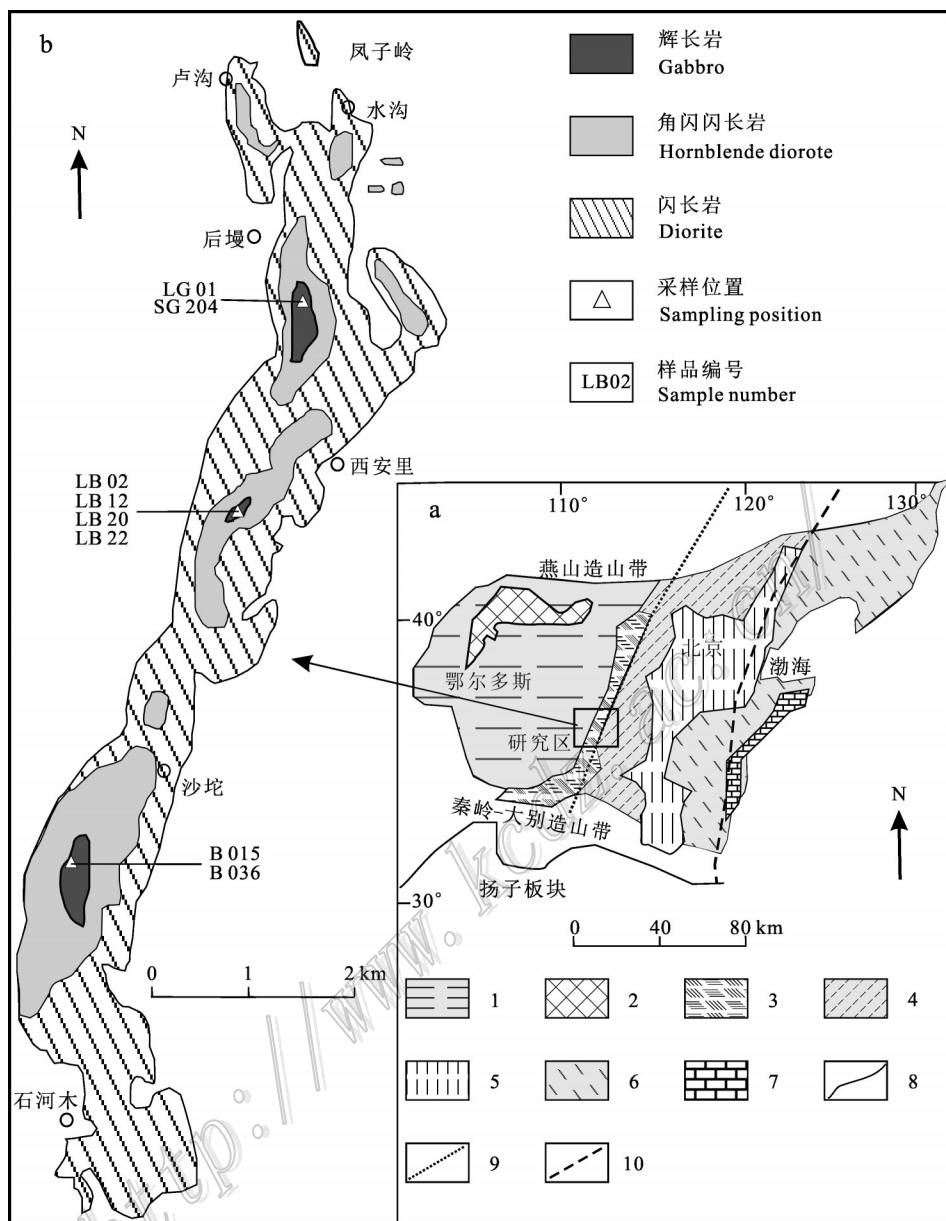


图1 南太行山平顺岩体大地构造位置简图(a)及地质简图(b)(据Zhao et al., 2000; 2001修改)

1—西部陆块;2—银川-河套裂谷带;3—山西-陕西裂谷带;4—中部造山带;5—华北裂谷带;6—东部陆块;7—苏-鲁超高压变质带;
8—构造单元界线;9—大兴安岭-太行山重力梯度带;10—郯庐断裂带

Fig.1 Tectonic location (a) and simplified geological map (b) of the Pingshun intrusions in the South Taihang Mountains
(modified after Zhao et al., 2000; 2001)

1—Western Block; 2—Yinchuan-Hetao Rift Zone; 3—Shanxi-Shaanxi Rift Zone; 4—South China orogen; 5—North China Rift Zone;
6—Eastern Block; 7—Su-Lu Hyperpressure metamorphism Zone; 8—Fectonic unit boundary; 9—Daxinganling-Taihang
gravity lineament; 10—Tan-Lu fault zone

量元素在长安大学自然资源部岩浆作用成矿与找矿重点实验室利用ICP-MS(USA Thermo Electron Co. X7型)测试,样品测试结果精度大于2%。Nd、Sr同位素测试工作在西北大学大陆动力学国家重点实验

室采用AG50W-8仪器完成,Nd同位素测试结果用 $^{146}\text{Nd}/^{144}\text{Nd} = 0.7219$ 的内检样品进行校正,Sr同位素测试结果用 $^{86}\text{Sr}/^{88}\text{Sr} = 0.1194$ 的内检样品进行校正,直到误差小于测试精度为止。

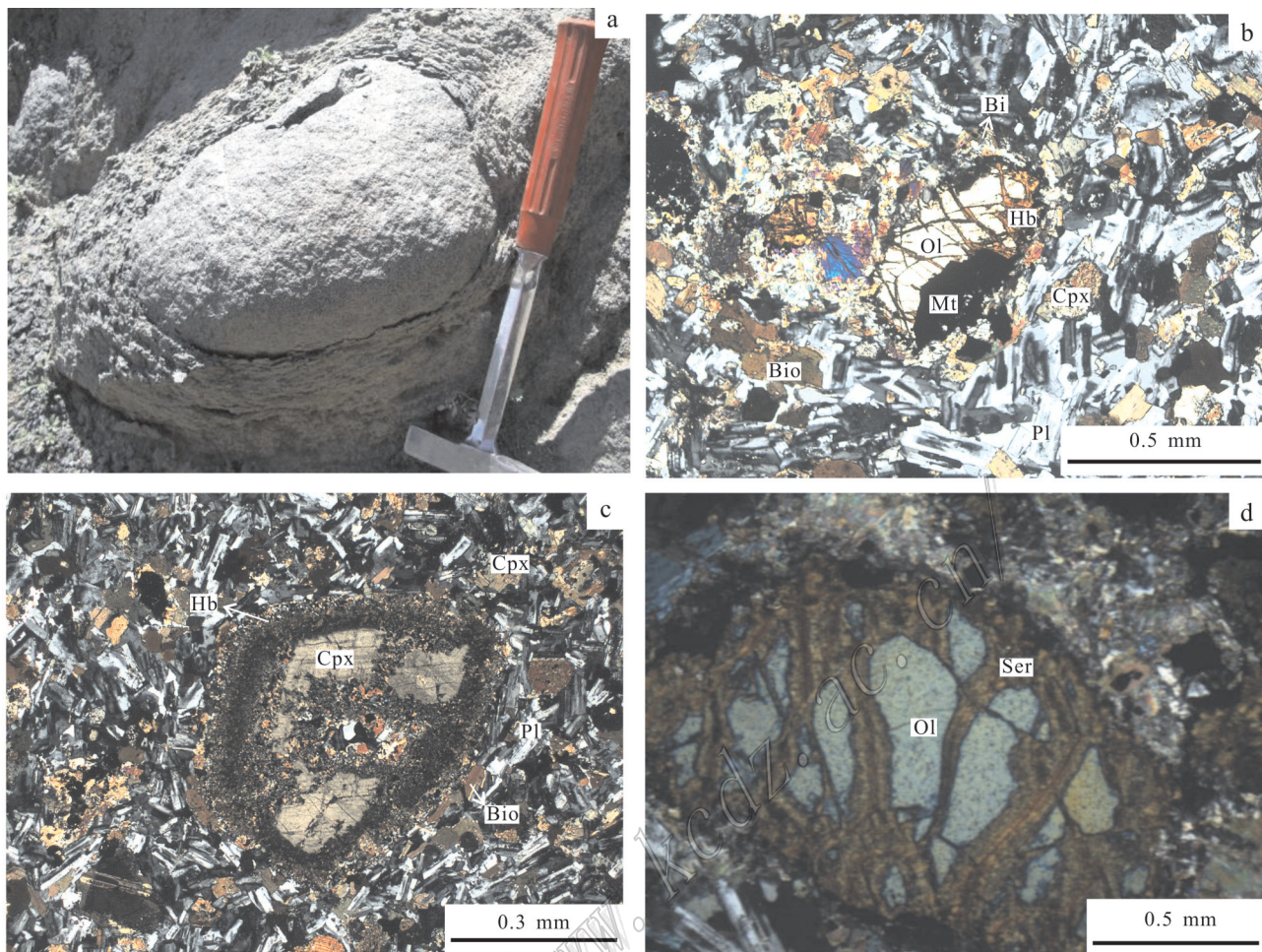


图2 平顺辉长岩体典型野外、显微照片

a. 平顺辉长岩体的球状风化；b. 辉长岩，由斜长石，单斜辉石，角闪石，黑云母，橄榄石和磁铁矿组成，橄榄石具有由黑云母和磁铁矿组成的反应边；c. 单斜辉石的反应边，由细粒角闪石和黑云母组成；d. 发育裂理的橄榄石，沿裂理发生蛇纹石化
Ol—橄榄石；Cpx—单斜辉石；Hb—角闪石；Pl—斜长石；Bi—黑云母；Q—石英；Mt—磁铁矿；Ser—蛇纹石

Fig. 2 Photos of field and microphotographs showing typical textures of the Pingshun gabbros

a. Spherical weathering of Pingshun gabbros; b. Gabbros, composed of plagioclase, clinopyroxene, hornblende, biotite, olivine and magnetite, olivine with reaction rim consisting of fine biotite and coarse magnetite; c. Clinopyroxene with a typical reaction rim, composed of fine hornblende and biotite; d. Olivine xenocryst with a typical embayed texture, note that olivine was altered to serpentine
Ol—Olivine; Cpx—Clinopyroxene; Hb—Hornblende; Pl—Plagioclase; Bi—Biotite; Q—Quartz; Mt—Magnetite; Ser—Serpentine

3 分析结果

3.1 SHRIMP 锆石 U-Pb 定年

本次研究对样品 LG01 所挑选出的锆石进行了 SHRIMP 锆石 U-Pb 年龄测试工作, 测试结果见表 1。从新鲜样品挑选出的锆石呈无色~浅黄色、透明, 自形~半自形, 大多为正方双锥状、长柱状、短柱状、半截锥状, 晶粒大小介于 70~950 μm 之间。在图 3a(锆

石阴极发光图)中, 锆石不具有典型的岩浆韵律环带结构。锆石晶体的长宽比值(3:1~3.5:1)以及锆石的 Th/U 比值(介于 1.03~1.92, 平均 1.42)显著高于变质锆石的 Th/U 比值(通常 < 0.1), 且 U-Th 质量分数图(图 3b)表现为较好的线性正相关, 锆石的上述特征表明锆石为岩浆成因, 且未经历后期的变质作用。本次工作共获得锆石 9 个分析点, $^{206}\text{Pb}/^{238}\text{U}$ 年龄变化范围较小, 介于 121.0~128.8 Ma, 且在谐和曲线图上数据成群分布(图 4a), 给出 $^{206}\text{Pb}/^{238}\text{U}$ 年龄的加权

表1 平顺辉长岩样品锆石 SHRIMP U-Pb 年龄分析结果表
Table 1 Zircon SHRIMP U-Pb analytical results of the Pingshun gabbros

点号	$w(\text{B})/10^{-6}$ U Th	$w^{(206\text{Pb})}/\%$	$^{232}\text{Th}/^{238}\text{U}$	$w^{(206\text{Pb}^*)}/10^{-6}$	比 值						$(^{206}\text{Pb}/^{238}\text{U})/\text{Ma}$	
					$^{207}\text{Pb}^*/^{206}\text{Pb}^*$	$\pm\%$	$^{207}\text{Pb}^*/^{235}\text{U}$	$\pm\%$	$^{206}\text{Pb}^*/^{238}\text{U}$	$\pm\%$		
LG01-1	0.54	556 747	1.39	9.09	0.0533	3.3	0.1389	3.9	0.01892	2.1	120.8	± 2.5
LG01-2	0.83	510 881	1.78	8.53	0.0462	5.3	0.1229	5.7	0.01930	2.2	123.2	± 2.6
LG01-3	1.17	601 926	1.59	10.20	0.0507	4.9	0.1372	5.3	0.01963	2.1	125.3	± 2.6
LG01-4	0.71	667 759	1.18	11.40	0.0500	4.7	0.1366	5.4	0.01982	2.5	126.5	± 3.2
LG01-5	0.30	499 926	1.92	8.37	0.0509	3.7	0.1366	4.3	0.01947	2.1	124.3	± 2.6
LG01-6	1.52	466 534	1.18	7.66	0.0431	9.0	0.112	9.3	0.01885	2.2	120.4	± 2.6
LG01-7	1.40	637 760	1.23	11.20	0.0469	7.7	0.130	8.0	0.02019	2.2	128.8	± 2.8
LG01-8	0.96	490 716	1.51	8.19	0.0456	6.4	0.1211	6.8	0.01928	2.1	123.1	± 2.6
LG01-9	1.63	619 619	1.03	10.20	0.0468	7.5	0.1221	7.8	0.01894	2.1	121.0	± 2.5

平均值为(123.4 ± 1.7)Ma(MSWD=1.10),代表了辉长岩体的形成年龄。

3.2 岩石地球化学特征

平顺辉长岩体代表性样品的主量、微量元素、稀土元素及Sr-Nd-Pb同位素测试结果见表2、表3。

平顺辉长岩的 $w(\text{SiO}_2)=42.82\% \sim 49.74\%$,平均值46.80%; $w(\text{Al}_2\text{O}_3)=11.91\% \sim 16.54\%$; $w(\text{MgO})=6.79\% \sim 14.57\%$; $w(\text{TiO}_2)=0.36\% \sim 1.53\%$; $w(\text{Fe}_2\text{O}_3^\text{T})=4.02\% \sim 15.03\%$; $w(\text{CaO})=7.45\% \sim 18.70\%$; $w(\text{K}_2\text{O})=0.18\% \sim 1.46\%$; $w(\text{Na}_2\text{O})=0.96\% \sim 3.38\%$; $\text{Na}_2\text{O} / \text{K}_2\text{O}=0.66 \sim 10.56$,平均值4.72, $\text{Mg}^{\#}$ ($\text{Mg}^{\#}=\text{Mg}/(\text{Mg}+\text{Fe})$)=56.53~81.68,均值63.23。在侵入岩的TAS分类图解(图5)中,所测样品落在橄榄辉长岩和辉长岩的范围内。在AFM图解(图6)中,所测样品的分布具有中等富铁的趋势,证明辉长岩岩石化学成分在结晶分异过

程中具有向拉斑玄武岩系列方向演化的特征,橄榄石、辉石发生了结晶分异作用。在 MgO 与其他氧化物图解(图7)中,随着 MgO 含量的递增, Al_2O_3 、 CaO 、 TiO_2 和 $\text{Fe}_2\text{O}_3^\text{T}$ 含量不断减少, SiO_2 含量不断增加, P_2O_5 、 K_2O 和 Na_2O 含量变化范围较小。

样品稀土元素质量分数为($59.5 \sim 109$) $\times 10^{-6}$,图8a中所有分析样品都表现出LREE富集,HREE和Y亏损($\text{LREE} / \text{HREE}=4.31 \sim 7.64$, $\text{La}_\text{N} / \text{Yb}_\text{N}=3.53 \sim 8.42$),微弱的正铕异常($\delta\text{Eu}=0.93 \sim 1.36$,平均为1.11),以及轻稀土元素和重稀土元素分异程度不明显的特征。

在图8b中,所有分析样品均表现出LREE、大离子亲石元素(如Sr、Ba、K)富集以及高场强元素(如Nb、Ta)亏损的特征。在Y-Sr/Y变异图解(图9)中,大多数岩石样品落入埃达克质岩石范围。过渡元素

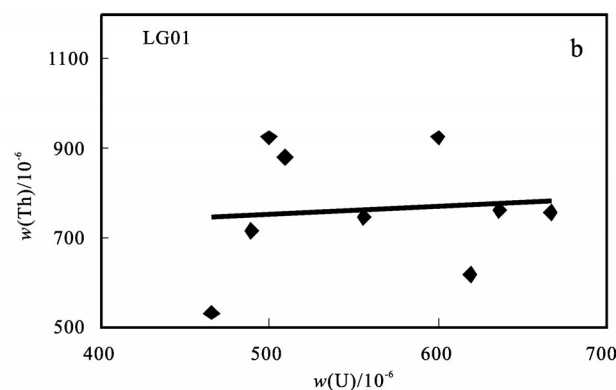
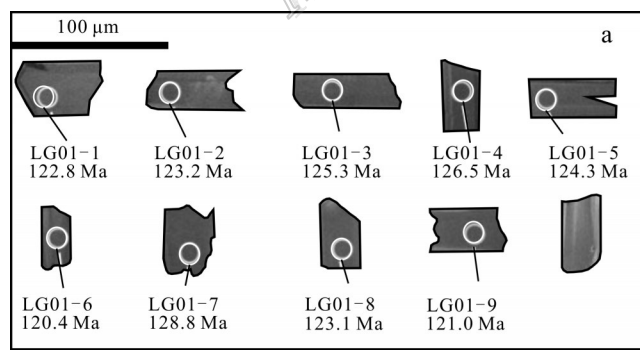


图3 平顺辉长岩(LG01)典型锆石的阴极发光图(a)和Th-U质量分数关系图(b)

Fig. 3 CL images (a) and Th-U content (b) of selected zircons from the Pingshun gabbros(LG01)

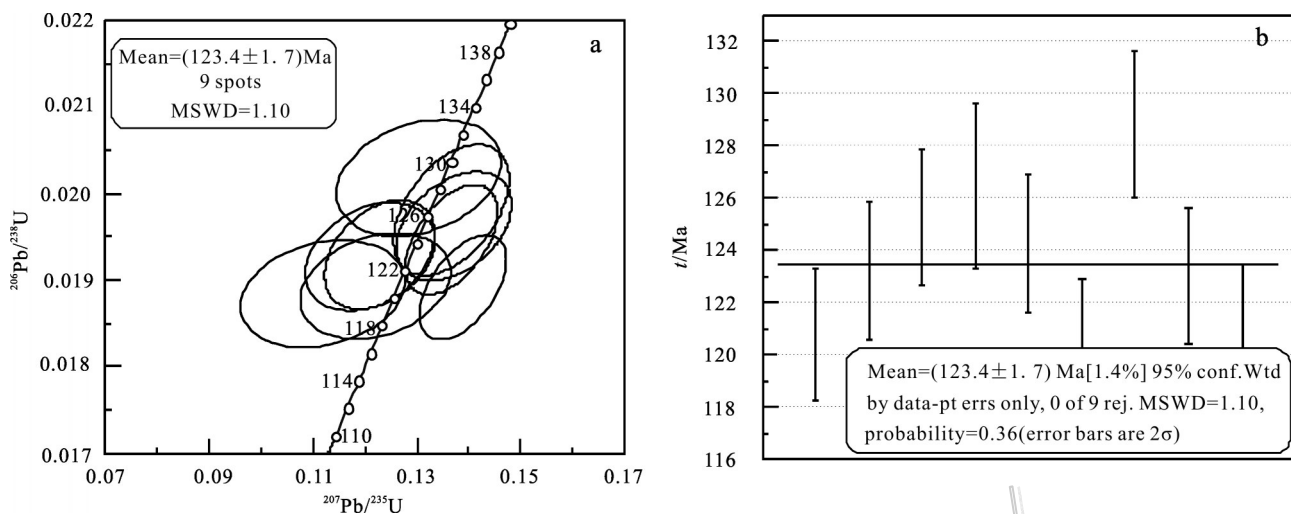
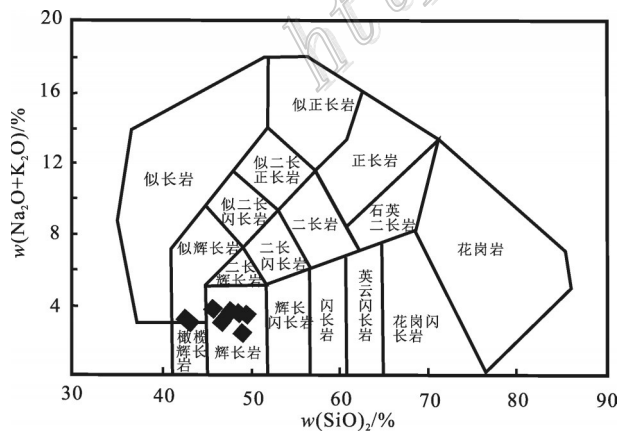


图4 平顺辉长岩SHRIMP锆石U-Pb年龄谐和图(a)和平均年龄图(b)

Fig.4 SHRIMP U-Pb concordia diagram (a) and average ages (b) of zircon from the Pingshun gabbros

$w(\text{Sc})$ 、 $w(\text{Cr})$ 、 $w(\text{Co})$ 、 $w(\text{Ni})$ 分别为 $5.90 \times 10^{-6} \sim 27.30 \times 10^{-6}$ 、 $19.04 \times 10^{-6} \sim 911.00 \times 10^{-6}$ 、 $11.20 \times 10^{-6} \sim 54.37 \times 10^{-6}$ 和 $16.80 \times 10^{-6} \sim 338.20 \times 10^{-6}$, 明显高于中国同类岩石的平均值(李昌年, 1992)。

平顺辉长岩的 $^{206}\text{Pb}/^{204}\text{Pb}=17.062 \sim 18.295$, $^{207}\text{Pb}/^{204}\text{Pb}=15.354 \sim 15.422$, $^{208}\text{Pb}/^{204}\text{Pb}=37.185 \sim 37.298$, $I_{\text{Sr}}=0.7046 \sim 0.7051$, $\varepsilon_{\text{Nd}}(125 \text{ Ma})=-14.15 \sim -13.00$ (表3), 显示具有富集地幔成因的特征。在 Pb 同位素图解(图 10a、b)中, 辉长岩样品都分布在 EM I 附近; 在 $^{87}\text{Sr}/^{86}\text{Sr}-\varepsilon_{\text{Nd}}(125 \text{ Ma})$ 图解(图 11a)中, 样品的 Sr、Nd 同位素组成相近, 较华北克拉通周缘造山带地区(太行、大别、方城等地区)中生代火山岩具有高 ε_{Nd}

图5 平顺辉长岩SiO₂-MgO变异图解(据Defant et al., 2001)Fig.5 SiO₂ versus MgO variation diagram of the Pingshun gabbros (after Defant et al., 2001)

和低 $^{87}\text{Sr}/^{86}\text{S}$ 比值(Chen et al., 2003; 陈斌等, 2005; Jahn et al., 1999; Fan et al., 2009; Zhang et al., 2002), 样品几乎全部都落入 EM I 范围内, 显示岩浆起源于 EM I 富集地幔的特征。

4 讨 论

4.1 岩体形成时代

平顺辉长岩体已有的年代学资料多为全岩或单矿物 K-Ar(170~175.08 Ma)(陈斌等, 2002; 刘建朝

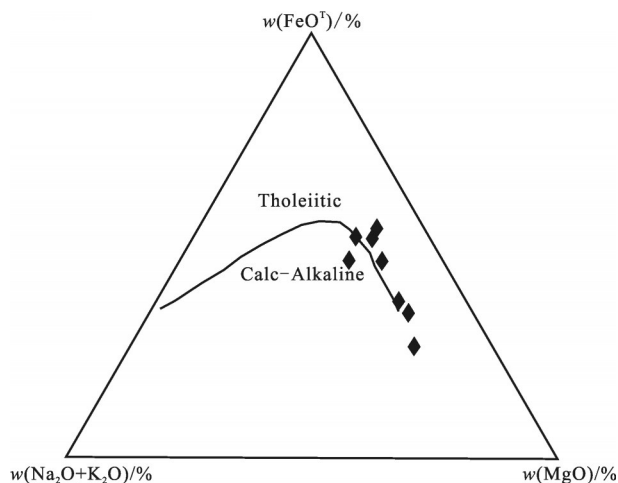


图6 平顺辉长岩AFM三角图解(图中分区据Irvine et al., 1971)

Fig.6 AFM diagram of the Pingshun gabbros (division after Irvin et al., 1971)

表2 平顺辉长岩样品主量元素、微量元素和稀土元素分析表

Table 2 Major elements, trace elements and rare earth elements compositions of the Pingshun gabbros

组分	LB02	LB12	LB20	LB22	LG01	SG204	B015	B036
<i>w(B)/%</i>								
SiO ₂	45.51	47.72	48.97	47.05	43.45	42.82	49.74	49.15
TiO ₂	1.32	0.82	0.36	1.16	1.53	1.49	0.6	0.77
Al ₂ O ₃	13.81	16.54	14.46	13.38	12.31	12.94	11.91	12.64
Fe ₂ O ₃ ^T	13.54	9.23	4.02	11.21	15.03	14.75	9.42	9.59
MnO	0.17	0.14	0.07	0.19	0.22	0.2	0.16	0.16
MgO	8.68	6.79	8.84	9.89	10.38	10.38	14.57	12.89
CaO	10.58	11.18	18.7	9.58	11.94	11.83	7.45	7.86
Na ₂ O	2.41	3.38	0.96	2.79	1.97	2.08	2.62	2.68
K ₂ O	1.4	0.32	1.46	0.18	0.98	1.16	0.92	1.00
P ₂ O ₅	0.39	0.32	0.02	0.15	0.31	0.35	0.26	0.30
LOI	2.95	3.76	2.2	4.69	1.33	1.31	2.26	2.49
总和	100.76	110.2	100.06	100.27	99.45	99.31	99.91	99.53
Mg [#]	56.52	59.87	81.68	64.15	58.35	58.80	75.83	73.16
<i>w(B)/10⁻⁶</i>								
Rb	11.67	3.923	29.52	1.481	9.066	14.28	15.05	18.59
Ba	854	127	934	54.29	362	383	413	439
Th	0.94	0.87	2.19	2.27	1.07	0.87	1.31	1.20
U	0.84	0.22	0.62	0.72	0.38	0.25	0.35	0.30
Ta	0.15	0.14	0.18	0.19	0.15	0.14	0.14	0.17
Nb	2.86	2.92	1.32	3.33	2.70	2.45	2.94	3.77
La	14.94	14.11	10.65	16.65	10.24	10.06	15.23	18.13
Ce	36.60	33.84	22.83	33.46	28.89	28.92	33.63	41.08
Sr	811.10	1275.00	311.10	578.40	728.50	675.00	649.70	661.00
Nd	24.56	20.43	11.67	18.18	24.36	23.97	18.63	25.27
Zr	52.82	60.00	159.20	100.70	43.71	41.06	64.44	67.77
Hf	1.85	1.89	3.88	2.60	1.64	1.55	1.81	2.08
Sm	5.83	4.12	2.38	3.80	6.17	6.00	3.58	4.78
Y	16.43	14.36	8.81	13.08	19.50	18.91	11.79	15.58
Cr	148	170	19.0	142.3	168.4	414.6	911	685.2
Co	35.09	28.03	14.16	11.20	42.18	45.83	54.37	52.19
Sc	17.97	24.18	5.90	13.57	16.21	18.38	25.03	27.30
Ni	36.76	60.93	16.80	28.48	76.8	214	338.2	275
La	14.94	14.11	10.65	16.65	10.24	10.06	15.23	18.13
Ce	36.60	33.84	22.83	33.46	28.89	28.92	33.63	41.08
Pr	5.08	4.48	2.83	4.11	4.62	4.61	4.30	5.58
Nd	24.56	20.43	11.67	18.18	24.36	23.97	18.63	25.27
Sm	5.83	4.12	2.38	3.80	6.17	6.00	3.58	4.78
Eu	2.37	1.54	1.14	1.43	2.23	2.24	1.13	1.48
Gd	5.96	4.29	2.73	3.89	6.22	6.22	3.69	4.91
Tb	0.82	0.60	0.36	0.55	0.91	0.88	0.42	0.56
Dy	4.32	3.29	1.89	2.97	4.75	4.68	2.49	3.34

续表 2

Continued Table 2

组分	LB02	LB12	LB20	LB22	LG01	SG204	B015	B036
$w(B)/10^{-6}$								
Ho	0.85	0.64	0.38	0.58	0.89	0.88	0.45	0.61
Er	2.34	1.84	1.14	1.71	2.46	2.40	1.35	1.75
Tm	0.29	0.25	0.17	0.23	0.31	0.30	0.20	0.26
Yb	1.88	1.64	1.19	1.59	1.95	1.83	1.22	1.61
Lu	0.27	0.25	0.19	0.25	0.27	0.25	0.19	0.23
Σ REE	106	91.3	59.5	89.3	94.2	93.2	86.5	109
LREE/HREE	5.34	6.13	6.39	6.59	4.31	4.35	7.64	7.27
La_N/Yb_N	5.36	5.79	6.02	7.06	3.53	3.71	8.42	7.61
La_N/Sm_N	1.61	2.15	2.82	2.75	1.05	1.06	2.68	2.39
Gd_N/Yb_N	2.56	2.11	1.85	1.97	2.57	2.74	2.44	2.47
δEu	1.22	1.11	1.36	1.13	1.09	1.12	0.95	0.93

注:比值单位为1。

等,2009)和全岩Rb-Sr(238 Ma)年龄(张海东,2011)。其中,K-Ar法主要采用角闪石、黑云母等含K较高的矿物,而Rb-Sr法要求岩石同源、同时、体系封闭,故2种方法所得年龄存在一定的争议性,这样的年代学资料严重制约了对南太行山中生代构造岩浆演化认识及对华北克拉通破坏机制的确定。

本论文获得样品LG01的SHRIMP锆石U-Pb年龄为(123.4 ± 1.7)Ma,其代表了平顺地区辉长岩体的形成年龄。该年龄与太行山其他地区的125~138 Ma岩浆活动、大别山岩浆活动126~137 Ma锆石U-Pb年龄相近(陈斌等,2005;Chen et al., 2003),说明

它们可能形成于同一个大地构造岩浆活动事件。

4.2 岩石成因

辉长岩体中的MgO与Al₂O₃、CaO、TiO₂、Fe₂O₃^T质量分数呈明显线性负相关,与SiO₂质量分数呈正相关,由于Fe、Mg、Ca和Ti主要赋存在橄榄石、辉石、铁钛氧化物中,所以Fe₂O₃^T、CaO、TiO₂、SiO₂与MgO之间的相关变化应该是由橄榄石、辉石和铁钛氧化物的分离结晶作用引起,这与其广泛产出橄榄石、辉石等反应残晶相吻合。Ba、Sr、LREE和大离子亲石元素相对富集,其含量明显高于在地壳中的平均含量,显示平顺辉长岩体的母岩浆含有大量来自

表3 平顺辉长岩样品Sr-Nd-Pb同位素分析表
Table 3 Sr-Nd-Pb isotopic data of the Pingshun gabbros

样品编号	$w(B)/10^{-6}$		$^{87}\text{Rb}/^{86}\text{Sr}$	$^{87}\text{Sr}/^{86}\text{Sr}$	$\pm 2\sigma$	I_{Sr} (125 Ma)	$w(B)/10^{-6}$		$^{147}\text{Sm}/^{144}\text{Nd}$
	Rb	Sr					Sm	Nd	
B036	15.05	649.7	0.067	0.705452	0.000012	0.704734375	3.58	18.63	0.1162
B015	18.59	661.0	0.081	0.705435	0.000014	0.704563886	4.78	25.27	0.1143
LG01	9.067	728.5	0.036	0.705453	0.000011	0.705067277	6.17	24.36	0.1530
LB022	18.59	661	0.081	0.705434	0.000012	0.704582774	5.83	24.56	0.1435
样品编号	$^{143}\text{Nd}/^{144}\text{Nd}$	$\pm 2\sigma$	$\epsilon_{\text{Nd}}(t)$ (125 Ma)	$^{206}\text{Pb}/^{204}\text{Pb}$	$^{207}\text{Pb}/^{204}\text{Pb}$	$^{208}\text{Pb}/^{204}\text{Pb}$	$(^{206}\text{Pb}/^{204}\text{Pb})_i$	$(^{207}\text{Pb}/^{204}\text{Pb})_i$	$(^{208}\text{Pb}/^{204}\text{Pb})_i$
B036	0.511840	0.000016	-12.9977024	18.474 ± 0.024	15.431 ± 0.021	37.374 ± 0.021	18.295	15.422	37.185
B015	0.511785	0.000007	-14.0278298	17.859 ± 0.021	15.429 ± 0.022	37.509 ± 0.018	17.679	15.42	37.298
LG01	0.511841	0.000016	-14.1531846	17.241 ± 0.002	15.363 ± 0.002	37.457 ± 0.004	17.062	15.354	37.229
LB022	0.511841	0.000016	-13.8578691	17.741 ± 0.003	15.413 ± 0.012	37.467 ± 0.002	17.562	15.404	37.253

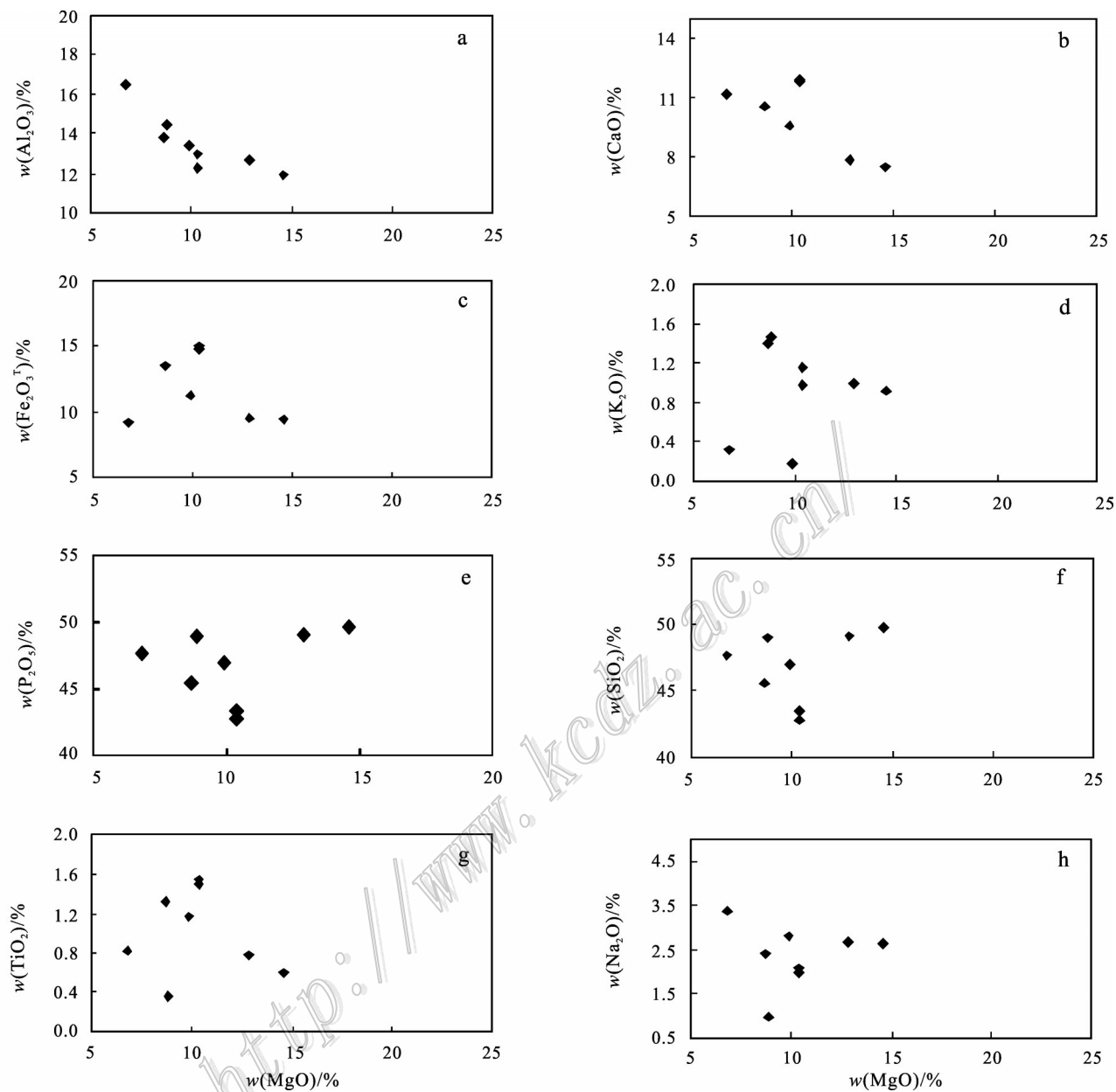


图7 平顺辉长岩体的MgO与其他氧化物图解

a. MgO与Al₂O₃图解; b. MgO与CaO图解; c. MgO与Fe₂O₃^T图解; d. MgO与K₂O图解; e. MgO与P₂O₅图解; f. MgO与SiO₂图解; g. MgO与TiO₂图解; h. MgO与Na₂O图解

Fig. 7 MgO versus other oxides for the Pingshun gabbros

a. MgO versus Al₂O₃ diagram; b. MgO versus CaO diagram; c. MgO versus Fe₂O₃^T diagram; d. MgO versus K₂O diagram; e. MgO versus P₂O₅ diagram; f. MgO versus SiO₂ diagram; g. MgO versus TiO₂ diagram; h. MgO versus Na₂O diagram

于富集地幔源区部分熔融的岩浆;显著亏损Ti、Nb、Ta等高场强元素说明岩浆在上升侵位过程中受到了地壳物质的混染。微弱的Eu正异常和亏损HREE特征,说明岩浆源区较深(大于60 km)(邓晋福等,1996; Menzies et al., 1998),斜长石处于不稳定区域,

没有发生大规模的斜长石分离结晶作用。在球粒陨石标准化(Tb/Yb)_N-(La/Sm)_N图解(Wang et al., 2002)中,辉长岩大部分样品落在尖晶石稳定域内,只有少数样品分布在石榴子石稳定域内。据Yang等(2007),岩石低La/Yb比值特征,显示壳幔发

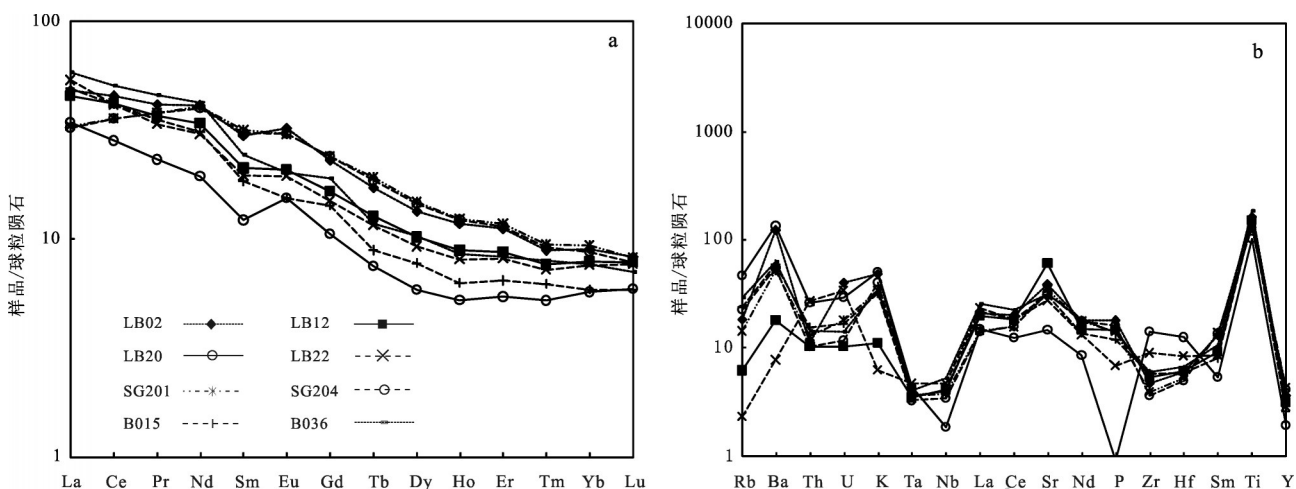


图8 平顺辉长岩体REE球粒陨石标准化配分图(a)和微量元素原始地幔标准化蛛网图(b)

(球粒陨石标准化值据 Tayloret al., 1985; 原始地幔标准化值据 Sun et al., 1989)

Fig. 8 The REE distribution patterns (a) and primitive mantle normalized incompatible element spidergram (b) of the Pingshun gabbros(chondrite values after Taylor et al., 1985; primitive mantle values from Sun et al., 1989)

生大部分熔融或处于尖晶石稳定状态；而高La/Yb比值显示部分熔融程度低或处于石榴子石稳定状态，而石榴子石稳定域与尖晶石稳定域的转换线对应形成深度约为80 km，相当于上地幔环境。

Mg[#]值常可以作为岩浆结晶分异的粗略指标，如果以60~71作为未分异的初始岩浆Mg[#]值(Langmuir et al., 1997)，那么平顺辉长岩Mg[#]=56.53~81.68(均值为63.23)就接近于原始岩浆。辉长岩Pb-Sr-Nd同位素组成特征(图10、图11)，显示岩浆起源富集地幔EMI。根据DePaolo(1981)的AFC模式，Sr-

Nd同位素模拟结果表明(图11a)，辉长岩体中混有10%左右的中-下地壳组分。

4.3 构造意义

华北克拉通自中生代以来，爆发了强烈的构造-岩浆-成矿活动，国内外大量文献显示该地区自中生代以来发生了大规模岩石圈减薄事件(Xu, 2001; Fan et al., 1992)，但对华北克拉通岩石圈减薄范围、动力学机制等问题仍存在较大争议。目前比较认可的观点是华北克拉通岩石圈减薄事件主要集中在135~115 Ma，减薄范围主要集中在山东地区，而太行山地区岩石圈减薄不明显且岩浆活动较早。本文研究表明平顺辉长岩体形成于123.4 Ma左右，与华北地区其他岩体形成年代一致，并具有与济南辉长岩、济阳盆地基性火山岩和北太行山辉长岩等相似的Sr-Nd同位素组成特征，这暗示平顺地区在早白垩世与华北地区具有相同的构造环境和地球动力学背景，即华北克拉通岩石圈减薄范围至少涵盖到南太行山地区(Fan et al., 1992; Griffinet al., 1992)。目前在太行山地区未发现来自软流圈地幔岩浆活动，而这种岩浆活动在济南、胶东等地区广泛分布，说明太行山地区岩石圈减薄相对较薄弱，另外，李松林等(2011)报道太行山东、西侧存在巨大差异，东侧薄(70~80 km)，西侧厚(85~120 km)，并且在西侧发现不同尺度的低速带，与此同时，太行山西侧鄂尔多斯盆地

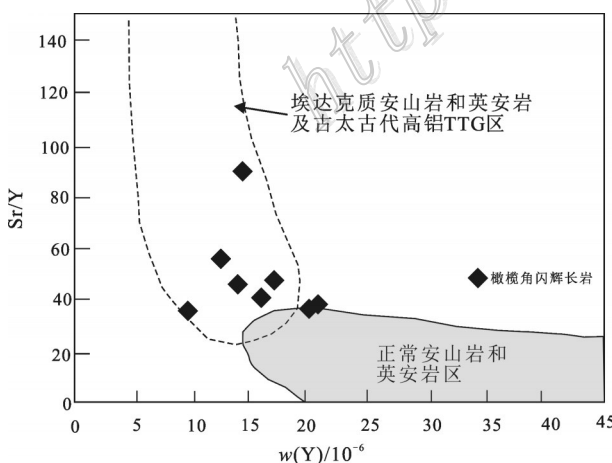


图9 平顺辉长岩Y-Sr/Y变异图解(据 Defant et al., 2001)

Fig. 9 Y-Sr/Y variation diagram of the Pingshun gabbros
(after Defant et al., 2001)

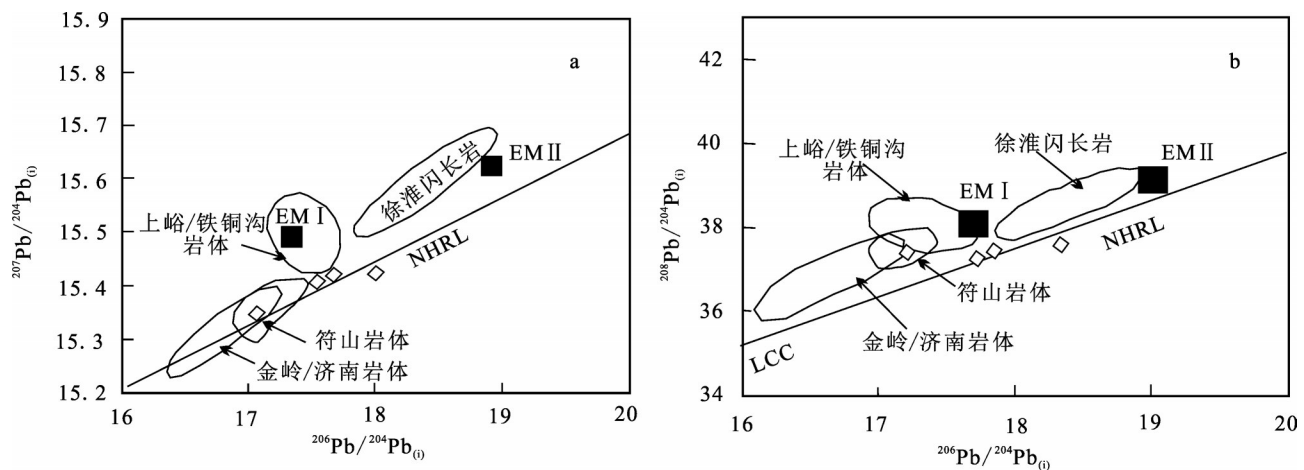


图10 Pb同位素相关曲线图解(杨学明等,2000)

a. $^{206}\text{Pb}/^{204}\text{Pb}$ - $^{207}\text{Pb}/^{204}\text{Pb}$ 图解; b. $^{206}\text{Pb}/^{204}\text{Pb}$ - $^{208}\text{Pb}/^{204}\text{Pb}$ 图解

济南/金岭岩体、符山岩体、上峪/铁铜沟岩体和徐淮闪长岩的Pb同位素数据来自许文良等,2009; Chen et al., 2004; NHRL—北半球参考线; LCC—大陆下地壳; EM I—I型富集地幔; EM II—II型富集地幔; EM I 和 EM II位置来自Zindler et al., 1986

Fig. 10 The correlation curves of isotope Pb (after Yang et al., 2000)

a. $^{206}\text{Pb}/^{204}\text{Pb}$ versus $^{207}\text{Pb}/^{204}\text{Pb}$ diagram; b. $^{206}\text{Pb}/^{204}\text{Pb}$ versus $^{208}\text{Pb}/^{204}\text{Pb}$ diagram

The Pb isotope data of Jinan/Jinling rock mass, Fushan rock mass, Shangyu/Fe-Cu rock mass and Xuhuai diorite after Xu et al., 2009;

Chen et al., 2004; NHRL—Northern hemisphere reference line; LCC—Continental lower crust; EM I—I enriched mantle;

EM II—II enriched mantle; EM I and EM II locations after Zindler et al., 1986

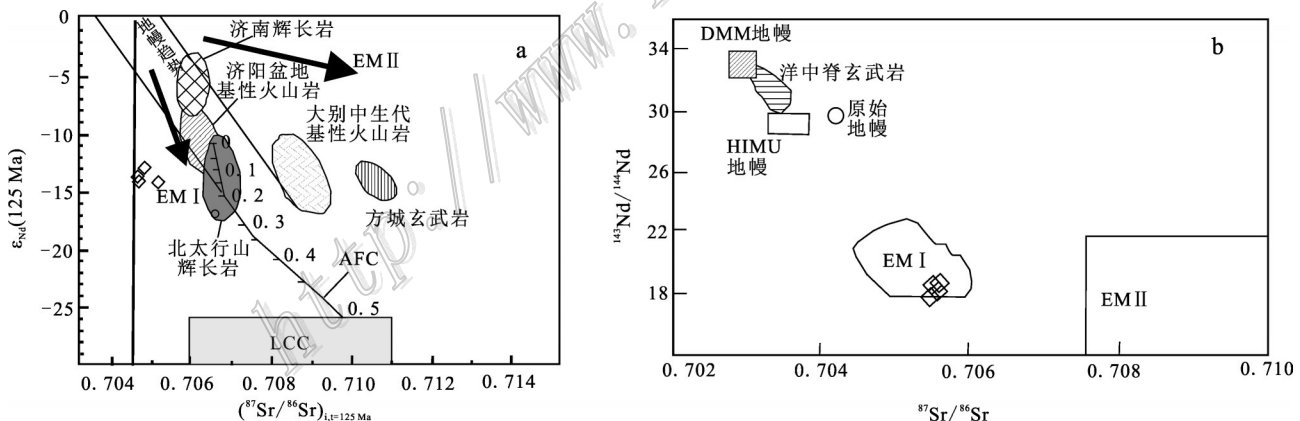


图11 平顺辉长岩Nd-Sr同位素图解

a. $^{87}\text{Sr}/^{86}\text{Sr}-\varepsilon_{\text{Nd}}(125 \text{ Ma})$ 图解; b. $^{87}\text{Sr}/^{86}\text{Sr}$ versus $^{143}\text{Nd}/^{144}\text{Nd}$ 图解

济阳盆地玄武岩、济南辉长岩、大别中生代基性火山岩和方城玄武岩的同位素数据来自Fan et al., 2001; Zhang et al., 2002; 2004; Jahn et al., 1999; 图11a中EM I、EM II和LCC的位置来自DePaolo, 1981; 图11b中DMM、EM I、EM II、HIMU和

原始地幔的位置来自Hart, 1984; Zindler et al., 1986

Fig. 11 Nd-Sr diagram of the Pingshun gabbros

a. $^{87}\text{Sr}/^{86}\text{Sr}$ versus $\varepsilon_{\text{Nd}}(125 \text{ Ma})$ diagram; b. $^{87}\text{Sr}/^{86}\text{Sr}$ versus $^{143}\text{Nd}/^{144}\text{Nd}$ diagram

The isotopic data of basalts in Jiayang Basin, gabbros in Jinan, Dabie Mesozoic volcanic rocks, and Fangcheng basalts after Fan et al., 2001;

Zhang et al., 2002; 2004; Jahn et al., 1999; the locations of EM I, EM II and LCC in Fig. 11a after DePaolo, 1981; DMM, EM I, EM II,

HIMU and primordial mantle in Fig. 11b after Hart, 1984; Zindler et al., 1986

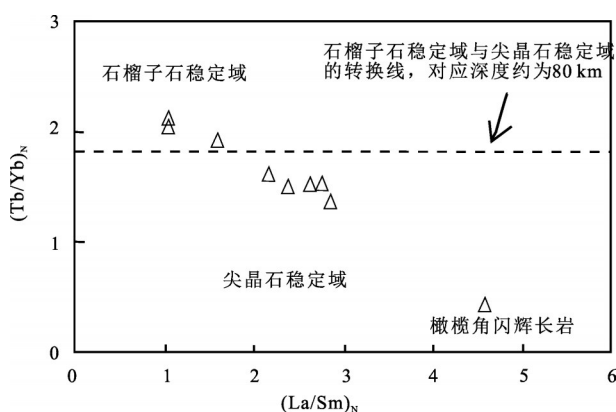


图 12 球粒陨石标准化 $(\text{Tb}/\text{Yb})_{\text{N}}$ - $(\text{La}/\text{Sm})_{\text{N}}$ 图解
(据 Yang et al., 2007)

Fig. 12 The chondrite-normalized $(\text{Tb}/\text{Yb})_{\text{N}}$ - $(\text{La}/\text{Sm})_{\text{N}}$ diagram (after Yang et al., 2007)

显示出较好的稳定性,因此,可将太行山重力梯度带作为华北克拉通岩石圈减薄的界限。

5 结 论

(1) 南太行山平顺辉长岩体 SHRIMP 锆石 U-Pb 年龄为 $(123.4 \pm 1.7)\text{ Ma}$, 与太行山其他地区基性、中酸性岩体形成年龄一致。

(2) 平顺辉长岩体具有低硅高镁,LREE 富集 HREE 亏损,微弱的正 Eu 异常,富集 LILE 元素,亏损 Nb-Ta 等高场强元素的特征。

(3) Sr-Nd-Pb 同位素研究显示,平顺辉长岩起源于 EM I 富集地幔,并受到微弱地壳物质混染,可能说明在早白垩世南太行山与华北克拉通一样发生了岩石圈减薄事件,具有统一的构造岩浆作用机制,且太行山可能是华北克拉通岩石圈减薄界限。

References

- Chen B, Zhai M G and Shao J A. 2002. Formation and significance of Mesozoic rock foundations in the northern segment of the Taihang Mountains: Evidence from major and trace element geochemistry[J]. Science in China (D), 32(11): 896-906 (in Chinese with English abstract).
- Chen B, Jahn B and Zhai M G. 2003. Sr-Nd isotopic characteristics of the Mesozoic magmatism in the Taihang-Yanshan Orogen, North China Craton, and implications for Archean lithosphere thinning[J]. Journal of the Geological Society, 160(6): 963-970.
- Chen B, Tian W, Zhai M G and Arakawa Y. 2005. Zircon U-Pb geochronology and geochemistry of Mesozoic magmatism in the Taihang Mountains and other areas in North China and their magmatism and geodynamic implications[J]. Acta Petrologica Sinica, 21: 13-24 (in Chinese with English abstract).
- Chen J F, Xie Z, Li H M, Zhang X D, Zhou X T, Park Y S, Ahn K S, Chen D G and Zhang X. 2003. U-Pb zircon ages for a collision-related K-rich complex at Shidao in the Sulu ultrahigh pressure terrane, China[J]. Geochemical Journal, 37: 35-46.
- Chen B, Jahn B M, Arakawa Y and Zhai M G. 2004. Petrogenesis of the Mesozoic intrusive complexes from the southern Taihang Orogen, North China Craton: Elemental and Sr-Nd-Pb isotopic constraints[J]. Contributions to Mineralogy and Petrology, 148: 489-501.
- Chen B, Tian W, Jahn B M and Chen Z C. 2008. Zircon SHRIMP U-Pb ages and in-situ Hf isotopic analysis for the Mesozoic intrusions in South Taihang, North China Craton: Evidence for hybridization between mantle-derived magmas and crustal components[J]. Lithos, 102: 118-137.
- Compston W, Williams I S and Mayer C. 1984. U-Pb geochronology of zircons from Lunar Breccia 73217 using a sensitive high resolution ion microprobe[J]. Journal of Geophysical Research, 89 (2) : 525-535.
- Defant M J and Kepezhinskas P. 2001. Evidence suggests slab melting in arc magmas[J]. Eos, Transactions American Geophysical Union, 82(6): 65-69.
- Deng J F, Zhao H L, Mo X X and Luo Z H. 1996. The key to the continental pillar structure in mainland China[M]. Beijing: Geological Publishing House. 1-115 (in Chinese with English abstract).
- Depaole D J. 1981. Trace element and isotopic effects of combined wallrock assimilation and fractional crystallization[J]. Earth and Planetary Science Letters, 53: 189-202.
- Fan W M and Menzies M A. 1992. Destruction of aged lower lithosphere and asthenosphere mantle beneath eastern China[J]. Geotectonica et Metallogenesis, 16(2): 171-180.
- Fan W M, Guo F, Wang Y J, Lin G and Zhang M. 2001. Post-orogenic bimodal volcanism along the Sulu Orogenic Belt in eastern China[J]. Physics and Chemistry of the Earth, Part A: Solid Earth and Geodesy, 26(9-10): 733-746.
- Fan W M, Guo F, Wang Y J and Zhang M. 2009. Late Mesozoic volcanism in the northern Huaiyang tectono-magmatic belt, Central

- China: Partial melts from a lithospheric mantle with subducted continental crust relicts beneath the DabieOrogen[J]? *Chemical Geology*,(209): 27-48.
- Griffin W L, O'Reilly S Y and Ryan C C. 1992. Composition and thermal structure of the lithosphere beneath South Africa, Siberia and China: Proton microprobe studies[C]. International Symposium on Cenozoic Volcanic Rocks and Deep-Seated Xenoliths of China and Its Environs:A65-A66.
- Griffin W L, Zhang A and O'Reilly S Y. 1998. Phanerozoic evolution of the lithosphere beneath the Sino-Korean Craton[J]. *Geodynamics Series*, 27: 107-126.
- Hart S R. 1984. A large-scale isotope anomaly in the southern Hemisphere Mantle[J]. *Nature*, 309: 735-757.
- Irvine I N and Baragar W R A. 1971. A guide to the chemical classification of the common volcanic rocks[J]. *Canadian Journal of Earth Sciences*, 8(5): 532-548.
- Jahn B M, Wu F, Lo C H and Tsai C H. 1999. Crust-mantle interaction induced by deep subduction of the continental crust: Geochemical and Sr-Nd isotopic evidence from post-collisional mafic-ultramafic intrusions of the northern Dabie complex, Central China[J]. *Chemical Geology*, 157: 119-146.
- Langmuir C. H, Bender J F and Bence A E. 1997. Petrogenesis of basalts from the famous area: Mid-Atlantic ridge[J]. *Earth Planetary Science Letters*, 36:133-156.
- Li C N. 1992. Geochemical methods for discriminating tectono-magmatic and their discussion[J]. *Geological Science and Technological Information*, 11(3):73-78(in Chinese with English abstract).
- Li S L, Lai X L, Liu B F, Wang Z Y, He J Y and Sun Y. 2011. Differences in lithospheric structure on both sides of the Taihang Mountains from inversion results of the Zhucheng-Yichuan artificial seismic section[J]. *Science China*, 41(5): 668-677 (in Chinese with English abstract).
- Liu J C, Zhang H D, Liu S W and Ge X H. 2009. Study on genesis of the intrusive complex in Pingshun area, southern Taihang Mountains[J]. *Geological Review*, 55(3): 318-328 (in Chinese with English abstract).
- Menzies M A and Xu Y. 1998. Geodynamics of the North China Craton[J]. *Geodynamics Series*, 27: 155-165.
- Song B, Zhang Y H, Wan Y S and Jian P. 2002. Zircon SHRIMP sample target production, age determination and discussion of related phenomena[J]. *Geological Review*, 48 (Supp.): 26-30 (in Chinese with English abstract).
- Sun S S and McDonough W F. 1989. Chemical and isotopic systematics of oceanic basalts: Implication for mantle composition and processes[A]. In: Saunders A D and Norry M J, eds. *Magmatism in the Ocean Basins*[C]. London: Geological Society Special Publication, 42:313-345.
- Taylor S R and Mc Lennan S M. 1985. The continental crust: Its composition and evolution[M]. London: Blackwell Scientific Publications, 1-312.
- Wang C G, Xu W L, Wang F and Yang D B. 2011. Origin of Early Cretaceous hornblende gabbro in Xi'anli, southern part of Taihang Mountains: Evidence of zircon U-Pb age, Hf isotope, and petrochemistry[J]. *Journal of University of Geosciences*, 36(3):471-482 (in Chinese with English abstract).
- Wang K, Plank T, Walker J D and Smith E I. 2002. A mantle melting profile across the Basin and Range, SW USA[J]. *Journal of Geophysical Research: Solid Earth*, 107:B1.
- Wang Y J, Fan W M, Zhang H F and Peng T P. 2006. Early Cretaceous gabbroic rocks from the Taihang Mountains: Implications for a paleo-subduction-related lithospheric mantle beneath the Central North China Craton[J]. *Lithos*, 86(3-4):281-302.
- Williams I S and Claesson S. 1987. Isotope evidence for the Precambrian province and Caledonian metamorphism of high grad paragneiss from the Seve Nappes, Scandinavian Caledonides. Ion microprobe zircon U-Th-Pb[J]. *Contributions to Mineralogy and Petrology*, 97: 205-217.
- Wu F Y, Ge W C, Sun D Y and Guo C L. 2003. Several problems in the study of lithosphere thinning in eastern China[J]. *Earth Science Frontier*, 10: 51-60 (in Chinese with English abstract).
- Wu F Y, Sun D Y, Zhang G L and Ren X W. 2006. On the deep geodynamic nature of the Yanshan movement[J]. *Geological Journal of Universities*, 6:379-388 (in Chinese with English abstract).
- Wu F Y, Xu Y G, Gao S and Zheng J P. 2008. The main academic debates on the study of the lithospheric thinning and craton damage in North China[J]. *Acta Petrologica Sinica*, 24(6): 1145-1174 (in Chinese with English abstract).
- Xu W L, Wang D Y, Gao S and Lin J Y. 2003. The discovery and significance of sandstone and pyroxenite inclusions in the Mesozoic Jinling diorite in Luxi[J]. *Chinese Science Bulletin*, 48 (8): 863-868 (in Chinese with English abstract).
- Xu W L, Yang D B, Ruan F P and Yu Y. 2009. The origin of the Fushan high-Mg diorite in the southern segment of the Taihang Mountains: The result of the reaction of melted melts of the submerged

- continental crust and the slow-buried peridotite[J]. *Acta Petrologica Sinica*, 25(8):1947-1961(in Chinese with English abstract).
- Xu W L, Wang C G, Wang F, Yang D B and Fu P P. 2010. Dunite xenoliths and olivine xenocrysts in Early Cretaceous Xi'anliHb-gabbros from southern Taihang Mountains: Constraints on nature of Mesozoic lithospheric mantle in Central China[J]. *Journal of Earth Sciences*, 21(5):692-710.
- Xu Y G. 2001. Thermo-tectonic destruction of the Archaean lithospheric keel beneath the Sino-Korean Craton in China: Evidence, timing and mechanism[J]. *Physics and Chemistry of the Earth, Part A: Solid Earth and Geodesy*, 26(9-10): 747-757.
- Xu Y G. 2007. Diachronous lithospheric thinning of the North China Craton and formation of the Daxin' anling-Taihangshan gravity lineament[J]. *Lithos*, 96 (1-2) : 281-297.
- Yang J H, Sun J F, Chen F, Wilde S A and Wu F Y .2007. Sources and petrogenesis of Late Triassic dolerite dikes in the Liaodong Peninsula: Implications for post-collisional lithosphere thinning of the eastern North China Craton[J]. *Journal of Petrology*, 48: 1973-1997.
- Yang X M, Yang X Y and Chen X Y. 2000. Rock geochemistry[M]. Hefei: University of Science and Technology of China Press. 50-214 (in Chinese with English abstract).
- Zhang H D. 2011. Diagenesis, mineralization and metallogenetic prediction of the Pingshun iron deposit in southern Shanxi (Ph.D. Thesis) [D]. Instructor: Liu J C. Xi'an: Chang'an University. 1-125 (in Chinese with English abstract).
- Zhang H F, Sun M and Zhou X H. 2002. Mesozoic lithosphere destruction beneath the North China Craton: Evidence from major, trace element, and Sr-Nd-Pb isotope studies of Fangcheng basalts[J]. *Contribution to Mineralogy and Petrology*, 144: 241-253.
- Zhang H F, Sun M, Zhou M F, Fan W M, Zhou X H and Zhai M G. 2004. Highly heterogeneous Late Mesozoic lithospheric mantle beneath the North China Craton: Evidence from Sr-Nd-Pb isotopic systematics of mafic igneous rocks[J]. *Geological Magazine*, 141: 55-62.
- Zhao G C, Cawood P A, Wilde S A, Sun M and Lu L Z. 2000. Metamorphism of basement rocks in the Central Zone of the North China Craton: Implications for Paleoproterozoic tectonic evolution[J]. *Precambrian Research*, 103(1-2):55-88.
- Zhao G C, Wilde S A, Cawood P A and Sun M. 2001. Archean blocks and their boundaries in the North China Craton: Lithological, geochemical, structural and *P-T* path constraints and tectonic evolution[J]. *Precambrian Research*, 107(1-2):45-73.
- Zindler A and Hart S. 1986. Chemical geodynamics[J]. *Annual Review of Earth and Planetary Sciences*, 14: 493-571.
- ### 附中文参考文献
- 陈斌, 翟明国, 邵济安. 2002. 太行山北段中生代岩基的成因和意义: 主要和微量元素地球化学证据[J]. *中国科学 D 辑*, 32(11): 896-906.
- 陈斌, 田伟, 翟明国, 荒川洋二. 2005. 太行山和华北其它地区中生代岩浆作用的锆石 U-Pb 年代学和地球化学特征及其岩浆成因和地球动力学意义[J]. *岩石学报*, 21: 13-24.
- 邓晋福, 赵海玲, 莫宣学, 罗照华. 1996. 中国大陆根柱构造——大陆动力学的钥匙[M]. 北京: 地质出版社. 1-115.
- 李昌年. 1992. 构造岩浆判别的地球化学方法及其讨论[J]. *地质科技情报*, 11(3):73-78.
- 李松林, 赖晓玲, 刘宝峰, 王志铸, 何加勇, 孙译. 2011. 由诸城-宜川人工地震剖面反演结果看太行山两侧岩石圈结构的差异[J]. *中国科学*, 41(5): 668-677.
- 刘建朝, 张海东, 刘淑文, 戈小红. 2009. 太行山南段平顺地区杂岩体成因研究[J]. *地质论评*, 55(3): 318-328.
- 宋彪, 张玉海, 万渝生, 简平. 2002. 锆石 SHRIMP 样品靶制作、年龄测定及有关现象讨论[J]. *地质论评*, 48 (增刊): 26-30.
- 王春光, 许文良, 王枫, 杨德彬. 2011. 太行山南段西安里早白垩世角闪辉长岩的成因: 锆石 U-Pb 年龄、Hf 同位素和岩石地球化学证据[J]. *中国地质大学学报*, 36(3):471-482.
- 吴福元, 葛文春, 孙德有, 郭春丽. 2003. 中国东部岩石圈减薄研究中的几个问题[J]. *地学前缘*, 10 : 51-60.
- 吴福元, 孙德有, 张广良, 任向文. 2006. 论燕山运动的深部地球动力学本质[J]. *高校地质学报*, 6 :379-388.
- 吴福元, 徐义刚, 高山, 郑建平. 2008. 华北岩石圈减薄与克拉通破坏研究的主要学术争论[J]. *岩石学报*, 24(6): 1145-1174.
- 许文良, 王冬艳, 高山, 林景仟. 2003. 鲁西中生代金岭闪长岩中纯橄榄岩和辉石岩包体的发现及其意义[J]. *科学通报*, 48(8):863-868.
- 许文良, 杨德彬, 裴福萍, 于洋. 2009. 太行山南段符山高镁闪长岩的成因——拆沉陆壳物质熔融的熔体与地慢橄榄岩反应的结果[J]. *岩石学报*, 25(8):1947-1961.
- 杨学明, 杨晓勇, 陈喜译. 2000. 岩石地球化学[M]. 合肥: 中国科学技术大学出版社. 50-214.
- 张海东. 2011. 晋南平顺铁矿床成岩成矿作用及成矿预测(博士论文)[D]. 导师: 刘建朝. 西安: 长安大学. 1-125.